THE JOURNAL OF PHYSICAL CHEMISTRY B

Article

pubs.acs.org/JPCB

Water Absorbed by Polyaniline Emeraldine Tends to Organize, Forming Nanodrops

Jordi Casanovas,[†] Manel Canales,[‡] Georgina Fabregat,[§,⊥] Alvaro Meneguzzi,[§,∥] and Carlos Alemán[§,⊥,*]

[†]Departament de Química, Escola Politècnica Superior, Universitat de Lleida, c/Jaume II n° 69, Lleida E-25001, Spain

[‡]Departament de Física i Enginyeria Nuclear, Facultat d'Informàtica, Universitat Politècnica de Catalunya, Jordi Girona 1-3, Barcelona E-08034, Spain

[§]Departament d'Enginyeria Química, E. T. S. d'Enginyeria Industrial de Barcelona, Universitat Politècnica de Catalunya, Diagonal 647, Barcelona E-08028, Spain

[⊥]Center for Research in Nano-Engineering, Universitat Politècnica de Catalunya, Campus Sud, Edifici C', C/Pasqual i Vila s/n, Barcelona E-08028, Spain

[∥]Departamento de Materiais, Escola de Engenharia, Universidade Federal do Rio Grande do Sul, Av. Bento Gonçalves, 9500, 91509-900, Porto Alegre, RS, Brazil

ABSTRACT: Interactions, in terms of both binding energies and microscopic organization, of water molecules absorbed by hydrophilic polyaniline emeraldine base have been investigated using quantum mechanical calculations, molecular dynamics simulation, FTIR spectroscopy, and ^{1}H NMR. From an enthalpic point of view, water molecules interact more favorably with imine nitrogen atoms than with amine ones, even though the latter are entropically favored with respect to the former because of their two binding sites. Quantum mechanical results show that interaction energies of water molecules reversibly absorbed but organized individually around a binding site range from 3.0 to 6.3 kcal/mol, which is in good agreement with activation energies of 3−5 kcal/mol previously determined by thermodynamic measurements. The irreversible absorption of water to produce C−OH groups in rings of diimine units has been examined considering a three steps process in which water molecules act as both acidic and nucleophilic reagent. Although calculations predict that the whole process is disfavored by 5−8 kcal/mol only, FTIR and ^{1}H NMR detected the existence of reversibly absorbed water but not of C−OH groups. Both the binding energies and the structural information provided by molecular dynamics simulations have been used to interpret the existence of two types of physisorbed water molecules: (i) those that interact individually with polymer chains and (ii) those immersed in nanodrops that are contained within the polymeric matrix. The binding energies calculated for these two types of water molecules are fully consistent with the thermodynamic activation energies previously reported.

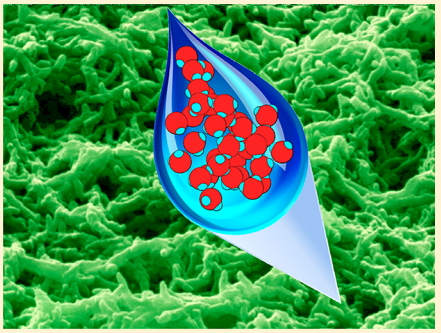

INTRODUCTION

Among conducting polymers, polyaniline (PAni) is currently of great interest for potential applications and also for the peculiar insulator−metal transition induced by protonation of backbone nitrogen sites.[1−3] The emeraldine base (EB) is the most interesting form of PAni due to its peculiar conducting properties under protonation of imine nitrogen atoms with a series of protonating acids.[1,4,5] Protonation leads to formation of the emeraldine salt (ES) with an increase in conductivity of a factor of 10^{10} despite unchanged electron number within each chain. Scheme 1 describes the chemical transformation of PAni-EB, which consists on phenylenediamine and quinoid diimine units (hereafter denoted AM and IM units, respectively), into PAni-ES. In addition to this chemical doping process, in which the protonic acid does not alter the oxidation state, PAni-EB can be electrochemically doped and dedoped by charge injection and removal, using techniques such as cyclic voltammetry.[6]

Scheme 1. Transformation of PAni-EB into PAni-ES

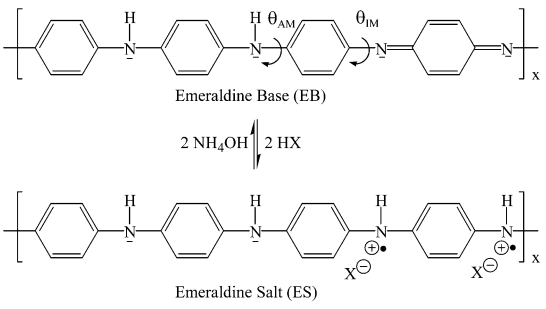

An interesting characteristic of PAni-EB is its ability to absorb water from humidity in air. The amount of water retained by this hydroscopic polymer depends on the ambient

Received: January 13, 2012
Revised: May 31, 2012
Published: June 12, 2012

conditions, annealing temperatures and time. This large dependence is reflected by the content of water reported by different authors using several experimental techniques (e.g., gravimetric analysis, TGA, DSC, NMR and elemental analysis), which was found to range from 5 to 15%.[7−13] In a very recent study we found that the maximum amount of water absorbed by both powder and film PAni-EB samples kept in chamber with relative humidity of around 100%, is 14%.[13]

Several hypothesis concerning the mechanism of water presence in PAni-EB samples have been proposed.[8,9,11] Water molecules are able to interact with amine and imine nitrogen atoms of AM and IM units, respectively. Water molecules participating in reversible absorption were categorized by Matveeva et al. in two types.[8,11] Molecules of the first type are hydrogen bonded to AM units with an activation energy of about 3−5 kcal/mol (Scheme 2a), mild treatments such drying

Scheme 2. Interaction of Reversibly Absorbed Water with (a) AM and (b) IM Units of PAni-EB. (c) Possible Structures Derived from the Hydrolysis of Imine Bond (Irreversibly Absorbed Water)

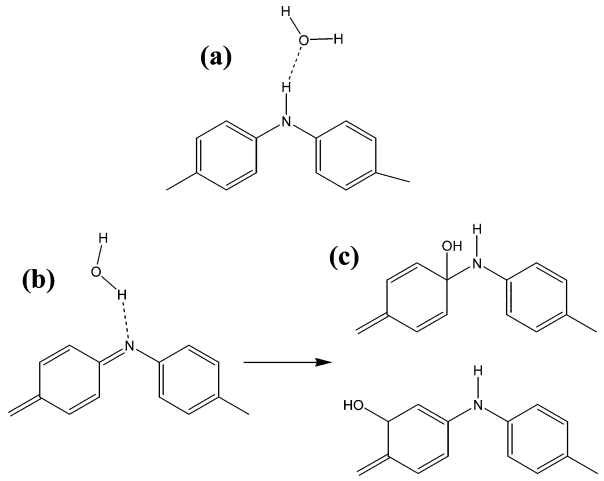

at 70 °C or at ambient temperature under dry nitrogen flux being enough to remove entirely them. The other corresponds to water molecules interacting with nitrogen atoms of IM units with a binding energy of about 15−18 kcal/mol (Scheme 2b). Accordingly, the interaction between the hydrogen atom of AM units in PAni-EB and the oxygen atom of water was assumed to be weaker than that between the hydrogen atom of water and the nitrogen atom of IM units. According to this hypothesis, water molecules attached by the second type of hydrogen bond could not escape from the polymeric matrix as those of the first type.[8,11] Canales et al. used atomistic Molecular Dynamics (MD) simulations to predict that the maximum content of water absorbed by PAni-EB corresponds to a concentration of 15% w/w, in excellent agreement with experimental evidence.[13] Analysis of the snapshots recorded from MD trajectories indicated that the hydration behavior of AM and IM units is similar.

On the other hand, irreversibly absorbed (chemically bonded) water molecules have been proposed to be involved in the hydrolysis of the C═N− imine bond (Scheme 2c). The possible existence of this hydrolysis process, would explain the existence of irreversibly absorbed water molecules observed by some authors.[8,11] As the energy of water absorption at the IM unit is sufficiently high, transformation among several configurations were assumed for chemically bonded water.

In this work, we use quantum mechanical calculations to examine the interaction of reversibly and irreversible absorbed water molecules with PAni-EB. In addition, the possible existence of irreversible absorbed water molecules has been experimentally examined using both FTIR and ^{1}H RMN. Finally, atomistic MD simulations have been carried out to investigate the microscopic organization of absorbed water molecules in the polymeric matrix. Results have allowed us to reinterpret the mechanism of water presence in PAni-EB, the new proposed mechanism being also fully consistent with previous experimental data.[8−13]

METHODS

Quantum Mechanical Calculations. Calculations on complexes formed by water molecules and a model oligomer blocked at the ends with amino groups were performed using the Gaussian 03[14] computer program. Geometry optimizations were carried out in the gas-phase using the B3LYP functional[15] combined with the 6-31+G(d,p) basis set.[16] Binding energies (ΔE_b), which were obtained applying the counterpoise (CP) method to correct the basis set superposition error,[17] were calculated as the difference between the total energy of the optimized complex and the energies of the isolated oligomer and water molecules.

Molecular Dynamics Simulations. PAni-EB has been represented considering a molecular model constituted by four chains of identical molecular weight, each one involving 25 a.m. and 25 IM units (Scheme 2) in an alternated disposition to retain the 3:1 benzenoid:quinoid rings ratio characteristic of PAni-EB, and 303 water molecules (i.e., 15% w/w). Amino-capped groups have not been used in this case due to both the lack of electronic effects in classical calculations and the fact that polymer chains are large enough. This model was found to be more stable than those made of chains with a random distribution of AM and IM units, and chains made exclusively of AM or IM units.[18] The amorphous and anisotropic nature of PAni-EB allows a satisfactory description of this material using a relatively small simulation box.[18,19] In all cases chains were blocked with a phenyl ring at the two ends. For computational efficiency reasons, C_6H_4 rings of both AM and IM units were represented using a pseudoatom model for C−H groups (united atom approximation). Thus, the total number of explicit particles contained in the simulated system was 4009.

Force-field parameters for PAni-EB were taken from our previous work,[18] while water was simulated considering the TIP3P model of Jorgensen and co-workers.[20] van der Waals interactions were represented using a standard 12−6 Lennard-Jones potential, an atom pair distance cutoff being applied at 10.0 Å. Electrostatic interactions were extensively computed by means of Ewald summations. The real space term was defined by the van der Waals cutoff, while the reciprocal space was computed by interpolation into an infinite grid of points (particle mesh Ewald) with maximum space grid points being 1.2 Å.[21]

Initial microstructure of hydrated PAni-EB was constructed by distributing randomly water molecules in sterically accessible positions located in a snapshot of PAni-EB, which was produced in our recent work (ρ= 1.245 g/cm^3).[18] MD simulations were performed using the GROMACS 4.2. program.[22−25] Before run the production MD trajectory, the starting microstructure was equilibrated using the following

dx.doi.org/10.1021/jp300426b | J. Phys. Chem. B 2012, 116, 7342−7350

Scheme 3. Position of Water Molecules around the EB Oligomers in Starting Configurations of EB-1H_2O/# Complexes, Where # Ranges from 1 to 6

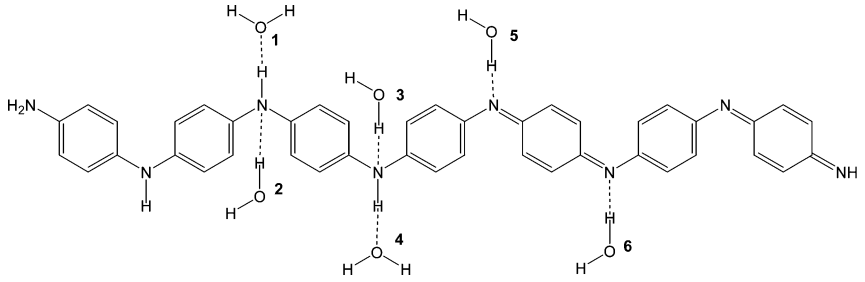

strategy: 1×10^4 steps of steepest descent energy minimization were performed in order to relax conformational and structural tensions. Next, different consecutive rounds of MD runs were performed in order to equilibrate the density, temperature, and pressure. First, water molecules were thermally relaxed by two consecutive runs, while polymer chains were kept frozen 0.5 ns of isothermal and 0.5 ns isobaric relaxation were run. After this, all atoms of the system were submitted to 0.15 ns of steady heating until the target temperature was reached (298 K), 5 ns of *NVT*-MD at 298 K (thermal equilibration) followed by 30 ns of density relaxation (*NPT*-MD). Both temperature and pressure were controlled by the weak coupling method of the Berendsen thermobarostat,[26] using a time constant for the heat bath coupling and a pressure relaxation time of 1 ps. After this, each *NPT*-MD production run at 300 K and 1 atm was 10 ns long. The numerical integration step was set to 1 fs while the coordinates of the production run was saved every 1000 steps (1 ps interval).

Synthesis of PAni-EB. PAni-ES was prepared according to the classical procedure, with amounts adjusted to allow the polymerization in a 5 L capacity double-walled reactor under controlled temperature and stirring. A solution consisting of oxidizing agent $[(NH_4)_2S_2O_8]$ (0.4 mol·L^{-1}) in HCl (1.5 mol·L^{-1}) was added slowly under constant stirring at −5 °C to a second HCl solution (1.5 mol·L^{-1}) containing aniline (0.4 mol·L^{-1}). The green powder, PAni-ES with density of 1.421 g·cm^{-3}, was filtered and exhaustively rinsed with distilled water in order to eliminate the excess of HCl and finally dried in an oven at 60 °C for 24 h.

PAni-EB, a dark blue powder was obtained after treatment of PAni-ES with a 0.5 mol·L^{-1} NH_4OH aqueous solution. The resulting emulsion was maintained at pH = 10 and under stirring for 6 h, the solid being finally dried in an oven at 60 °C for 24 h.

FTIR Spectroscopy. IR absorption spectra were recorded on a FTIR Jasco 4100 spectrometer. Samples were placed in an attenuated total reflection accessory (Top-plate) with a diamond crystal (Specac model MKII Golden Gate Heated Single Reflection Diamond ATR). For each sample 32 scans were performed between 4000 and 600 cm^{-1} with a resolution of 4 cm^{-1}.

NMR Measurements. ^{1}H NMR spectra were measured on a Bruker AM-300 WB spectrometer operated at 300.13 MHz. Measurements were performed on samples of PAni-EB (5 mg) dissolved in 1.0 mL of deuterated dimethyl sulfoxide (DMSO-d_6). Because of the partial solubility of PAni-EB, all samples were filtered before measurements. All chemical shifts are expressed in parts per million relative to the methyl carbon resonance of tetramethylsilane (TMS).

RESULTS AND DISCUSSION

Energetic Analysis of Reversibly Absorbed Water Molecules. Molecular geometries of six complexes formed by a single water molecule and a model oligomer of PAni-EB, denoted EB, were optimized at the B3LYP/631+G(d,p) level. The chemical structure of EB, which is displayed in Scheme 3, was designed to get the maximum information about the binding of AM and IM binding sites with individual water molecules. Specifically, the EB model was selected by the following reasons: (i) it is large enough to avoid undesirable end effects in the evaluation of the binding energies between AM or IM units and water molecules, amino capped groups mimicking the continuity of the polymer chain better than simple phenyl rings; (ii) although its block structure is unrealistic, it permits one to separate the contributions associated with a given type of binding site (AM or IM), avoiding the interferences induced by the other; (iii) despite its limitations, the use of one model oligomer only permits a direct comparison of calculated energies. We are fully aware that this model oligomer does not satisfy the 3:1 benzenoid:quinoid rings ratio experimentally found in PAni-EB. However, considering that the aim of the quantum mechanical calculations presented in this section is to get information about the interaction of individual water molecules and a given binding site (i.e., binding energy and hydrogen bonding parameters) and that we are representing a PAni-EB as a small oligomer in the gas-phase, the relative importance of this limitation looks small.

Scheme 3 also depicts the position of water molecules at starting configurations, resulting complexes being denoted as EB-1H_2O/# where # is the label used to identify each water molecule. As it can be seen, water molecule interacts with an AM unit in four complexes (# = 1 to 4) while the interaction occurs with an IM unit in the remaining two (# = 5 and 6). It is worth noting that all complexes involved conventional hydrogen bonding interactions, complexes with $\pi\cdots$H−O interactions being omitted in the present study. This is because the latter interaction is much less representative, in terms of binding energy and population, than conventional hydrogen bonds.

Table 1 lists the binding energies (ΔE_b) of the six EB-1H_2O/# complexes. The binding energies of the four complexes with $H_2O\cdots$AM interactions range from −3.0 to −4.5 kcal/mol. Detailed inspection of these values together with Figure 1, which displays the position of water molecules after geometry optimization, reflects that the strength of the interaction in complexes where the AM nitrogen acts as a hydrogen bonding donor (EB-1H_2O/# with # = 1 and 4; Figure 1a) is around 1 kcal/mol lower than that of complexes where AM units act as

dx.doi.org/10.1021/jp300426b | *J. Phys. Chem. B* 2012, 116, 7342−7350

Table 1. Relative Energy[a] (ΔE, in kcal/mol), Binding Energy (ΔE_b, in kcal/mol) and Intermolecular Hydrogen Bonding Parameters (Distances and Angles in Å and deg, Respectively) Calculated at the B3LYP/6-31+G(d,p) Level for EB-1H_2O/# (with # Ranging from 1 to 6) and EB-2H_2O/(#,#′) (with #,#′ = 1,4; 2,3; and 5,6) complexes[b]

complex	ΔE	ΔE_b	H···O	∠N−H···O	H···N	∠O−H···N
EB-1H_2O/1	2.2	−4.1	2.054	174.9	–	–
EB-1H_2O/2	2.7	−3.7	–	–	2.005	172.9
EB-1H_2O/3	3.3	−3.0	–	–	2.038	167.8
EB-1H_2O/4	1.8	−4.5	2.038	177.1	–	–
EB-1H_2O/5	0.0[c]	−6.3	–	–	1.918	174.7
EB-1H_2O/6	0.0	−6.3	–	–	1.926	173.7
EB-2H_2O/(1,4)	3.8	−8.6	2.056	174.0		
			2.040	177.0		
EB-2H_2O/(2,3)	5.7	−6.6			2.025	170.9
					2.037	167.4
EB-2H_2O/(5,6)	0.0[d]	−12.3			1.925	176.0
					1.925	174.2

[a]The BSSE of the energies have been corrected by applying the CP method. [b]The position of the water molecules is depicted in Scheme 3. [c]E = −2135.460232 au. [d]E = −2211.903776 au.

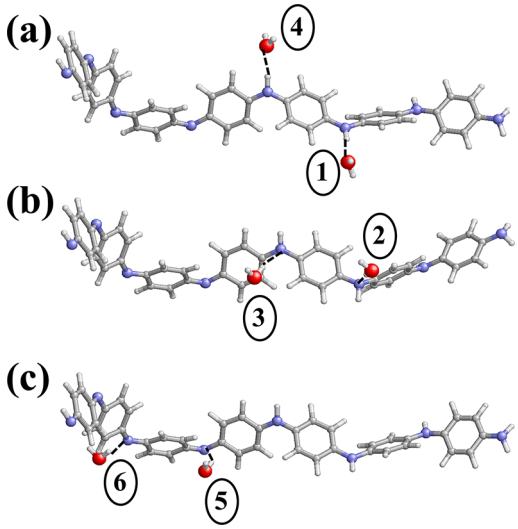

Figure 1. Position of water molecules with respect to nitrogen atoms in the minimum energy conformations of the six EB-1H_2O/# complexes: (a) water molecules in complexes with # = 1 and 4, where AM units act as hydrogen bonding donors; (b) water molecules in complexes with # = 2 and 3, where AM units act as hydrogen bonding acceptors; (c) water molecules in complexes with # = 5 and 6, where IM units act as hydrogen bonding acceptors. Hydrogen bonds are indicated by dashed lines.

hydrogen bonding acceptors (EB-1H_2O/# with # = 2 and 3; Figure 1b). These values are in excellent agreement with thermodynamic results described by Mateeva et al.,[8,11] who reported that the activation energy of water molecules absorbed at AM units is 3−5 kcal/mol.

The binding energies of the two complexes with H_2O···IM interactions (EB-1H_2O/# with # = 5 and 6; Figure 1c) are identical, −6.3 kcal/mol. The latter value reflects that reversibly absorbed water molecules interact more favorably with IM units than with AM ones, as was experimentally found.[8,11] However, the activation energy attributed to water molecules interacting with IM units, 15−18 kcal/mol,[8,11] is significantly overestimated with respect to the calculated binding energies. On the other hand, relative energies defined with respect to the most stable complex (ΔE) and intermolecular hydrogen bonding parameters, which are included in Table 1, are fully consistent with strength of H_2O···AM and H_2O···IM interactions.

The three structures displayed in Figure 1 were used as starting points for geometry optimization of complexes involving two water molecules with identical interaction patterns. These complexes have been denoted EB-2H_2O/(#,#′), where (#,#′) are the labels that allow identify water molecules according to Scheme 3, i.e., (#,#′) = (1,4), (2,3) and (5,6) refer to the patterns in which AM units act as hydrogen bonding donor, AM units act as hydrogen bonding acceptor and IM units act as hydrogen bonding donor, respectively. The positions of the two water molecules in optimized EB-2H_2O/(#,#′) complexes (not shown) were very similar to those displayed in Figure 1 for EB-1H_2O/# complexes, which was attributed to the lack of significant H_2O···H_2O interactions. Relative energies, binding energies and hydrogen bonding parameters for the three EB-2H_2O/(#,#′) complexes are included in Table 1. As it can be seen, the binding energy calculated for each EB-2H_2O/(#,#′) complex is the sum of the binding energies obtained for the corresponding EB-1H_2O/# and EB-1H_2O/#′ complexes, evidencing the absence of any cooperative effect between different interacting units.

In spite of the fact that H_2O···IM interactions are energetically favored with respect to H_2O···AM ones, the two types of interactions are expected to be present with similar frequencies in hygroscopic PAni-EB samples saturated with absorbed water. This is because the favorable enthalpic effect associated with H_2O···IM interactions is compensated by the entropic term, which favors H_2O···AM interactions due to their two interaction modes. This behavior was satisfactorily predicted by classical MD simulations.[13] Thus, comparison of the partial distribution functions calculated for AM···O and IM···O pairs, where O represents the oxygen of water, indicated that the hydration behavior of AM and IM units was similar.

Quantum mechanical results displayed in Table 1 suggest a reinterpretation of the thermodynamic activation energies determined by Mateeva et al.[8,11] Those authors determined calorimetrically activation energies of about 3−5 and 15−18 kcal/mol, which were attributed to water molecules interacting with AM and IM units, respectively. However, quantum mechanical results indicate that the activation energy of 3−5 kcal/mol corresponds to reversible absorber water molecules organized individually around either amine or imine nitrogen binding sites. Accordingly, the activation energy of about 15−18 kcal/mol should be identified with irreversibly absorbed water molecules or with a complex organization of reversible absorbed water molecules.

Energetic and Experimental Analyses of Irreversibly Absorbed Water Molecules. Consideration of irreversible absorption of water is based on the reactive ability of imine nitrogen atoms, which may capture a proton from an acid to generate an intermediate protonated structure stabilized through delocalization of the positive charge (step A in Scheme 4). The interaction of the active center of such protonated specie with a water molecule, which acts as a nucleophilic reagent, results in an intermediate specie (step B in Scheme 4) that transforms into the final product of hydration after removal

dx.doi.org/10.1021/jp300426b | J. Phys. Chem. B 2012, 116, 7342−7350

Scheme 4. Processes Examined To Study the Irreversible Absorption of Water by PAni-EB, Which Are Based on the Action of Water as both Acidic and Nucleophilic Reagent

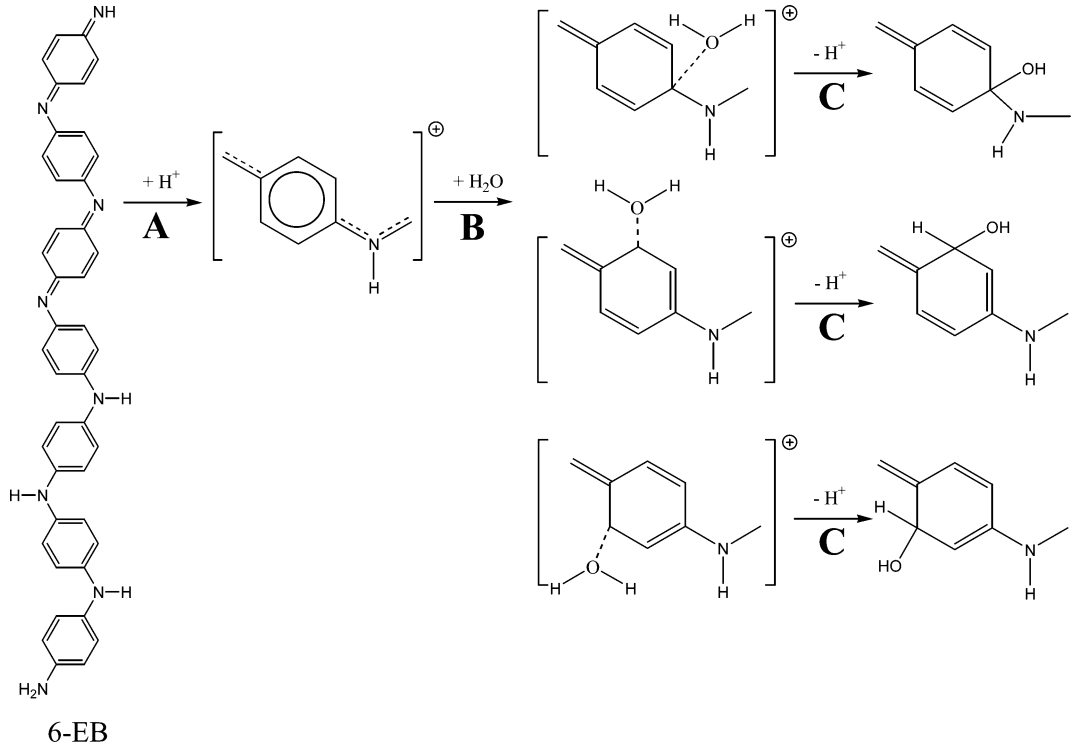

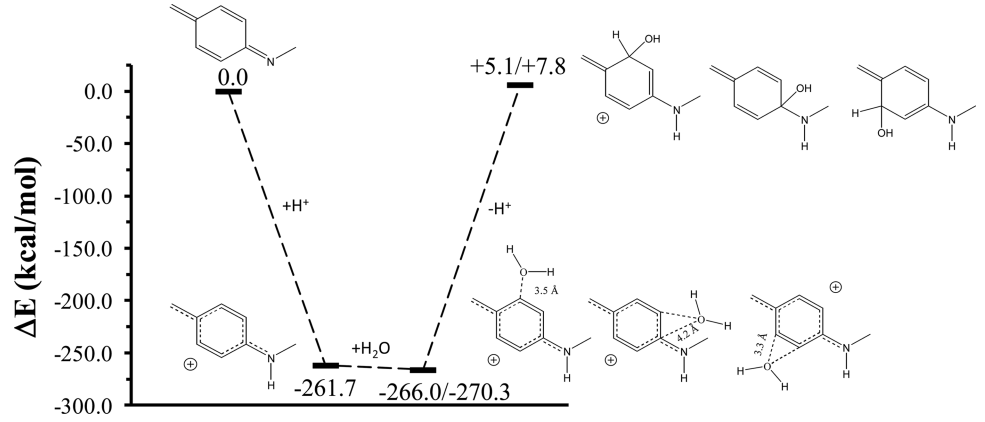

Figure 2. Energy diagram associated with the irreversible absorption of water (see Scheme 4). Energies are relative to EB. The energies given for the species resulting from the nucleophilic attack of water and deprotonation refer to the interval obtained for the depicted species.

of protons (step C in Scheme 4). Matveeva[11] proposed this mechanism assuming that a water molecule itself may act as some acidic reagent in absence of a protonic electrolyte. Specifically, such author proposed the dissociation of water at the imine center through the reaction $N(HOH) \leftrightarrows N^{+}H(OH)^{-}$ and the subsequent development of the hydration process according to steps B and C of Scheme 4.[11]

The energetic associated with A → B → C processes has been calculated at the B3LYP/631+G(d,p) level, results being displayed in Figure 2a. As it can be seen, the protonation of EB is an exotermic process, the favorable energy found for A being similar to those reported for the protonation of the nitrogen atom in other aromatic compounds.[27] The energy associated with B has been determined with respect to the different calculated complexes, whose structures are schematically displayed in Figure 2. As it can be seen, in this complex the water molecule interacts simultaneously with two hydrogen atoms, producing an energy gain that ranges from 4.3 to 8.6 kcal/mol. These values are similar to the hydrogen bonding energies displayed in Table 1. Finally, the products obtained after the nucleophilic attack of water and subsequent deprotonation are unfavored in by 5−8 kcal/mol.

Figure 3 compares the FTIR spectra of PAni-EB samples after (a) one night kept in an oven at 70 °C (dehydrated sample), (b) 2 days in a closed chamber with relative humidity at around 100%, which was achieved through a warm water bath (wet-I sample), and (c) 2 weeks in a closed chamber with relative humidity at around 100% (wet-II sample). Detailed assignment of absorption peaks was previously reported in the literature and, therefore, has not repeated here.[28−30] Accordingly, the discussion has been focused on differences due to the reversible and irreversible absorption of water.

dx.doi.org/10.1021/jp300426b | J. Phys. Chem. B 2012, 116, 7342−7350

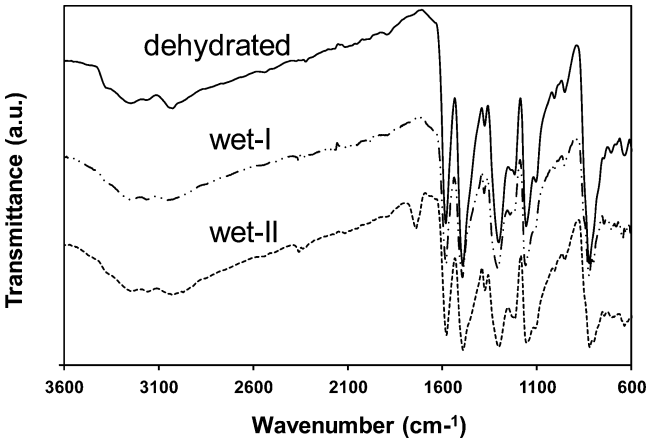

Figure 3. FTIR spectra of PAni-EB samples after one night kept in an oven at 70 °C (dehydrated) and 2 days (wet-I) and 2 weeks (wet-II) in a closed chamber with relative humidity at around 100%.

As is evidenced in Figure 3, there is no significant difference between the spectra of the three samples in the 600−1700 cm^{-1} interval. Identification of the C−O stretching (1050−1150 cm^{-1}, strong), which could be formed by the irreversible absorption of water, is unfortunately not possible because the position of its band overlaps that of the absorption peaks typically assigned to C−H in plane bending (1060−1162 cm^{-1}, strong) and ring deformation (1103 cm^{-1}, shoulder) of PAni-EB.[28−31] The appearance of an absorption peak at 1748 cm^{-1} in the wet-II sample is consistent with the formation of C═O groups through oxidative degradation processes during the prolonged treatment in the closed chamber with a relative humidity of 100%. On the other hand, absorption peaks and shoulders at 3387 and 3257 are typically assigned to asymmetric and symmetric NH_2 stretching vibrations, respectively, while the 3033 cm^{-1} corresponds to the stretching vibrations of aromatic CH groups.[30] The peak at 3169 cm^{-1} is usually associated with the ═NH stretching,[30] even though it has been recently related with the O−H stretching of water molecules physisorbed into the PAni-EB backbone (i.e., reversibly absorbed water).[33] In spite of this overlapping, we consider that contribution of water to such signal is very possible since its intensity grows as follows for the different samples: dehydrated < wet-I < wet-II. Finally, it should be mentioned that the O−H stretching of hydrogen bonded C−OH alcohol groups is expected to appear as a strong peak in the 3200−3600 cm^{-1} interval. Although the overall of these results suggest the presence of reversibly absorbed water, the FTIR technique does not allow us to discern about the existence of irreversibly absorbed water.

Figure 4 reports the ^{1}H NMR spectrum of the wet-I PAni-EB sample dissolved in DMSO-d_6. Signals at 8.2 and 7.0 ppm have been attributed to the NH and Ar−H groups,[32] respectively, while peaks at 3.35 and 2.50 ppm correspond to water molecules reversibly absorbed by the polymer after two days in a humid environment and DMSO, respectively. On the other hand, analysis of the ^{1}H NMR spectrum of *m*-anilinophenol in DMSO, which is reported in the Spectral Database for Organic Compounds[33] (SDBS), indicates that the shift expected for the C−OH signal is around 9.2 ppm. The lack of any peak at such region indicates that water molecules have not been irreversibly absorbed through the mechanism displayed in Scheme 4.

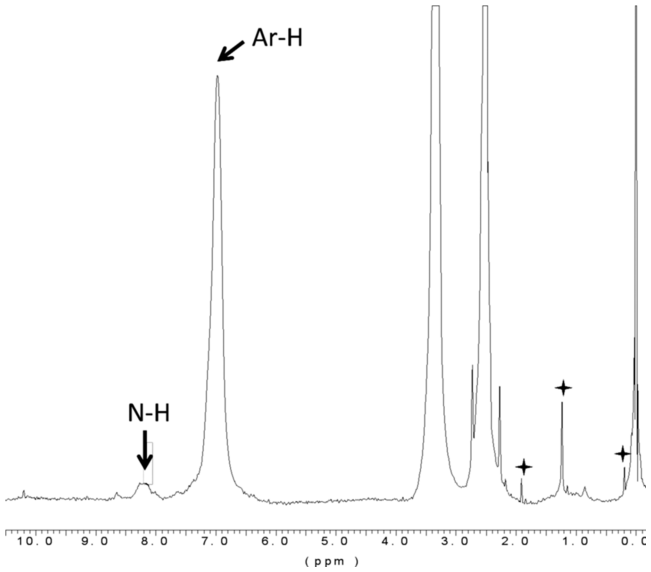

Figure 4. 300 MHz ^{1}H NMR spectrum in DMSO-d_6 of PAni-EB after 2 days in a closed chamber with relative humidity at around 100%. Impurities associated with the sample are marked with an asterisk.

Organization of Water Molecules and Nanodrops in Bulk PAni-EB. The organization of reversibly absorbed water molecules has been investigated using MD simulations. It should be mentioned that the force-field used to represent PAni-EB was parametrized to reproduce the experimental density and amorphous structure[21] but not the interaction of PAni-EB with water molecules. Therefore, results derived in this section should be considered qualitatively only. Figure 5

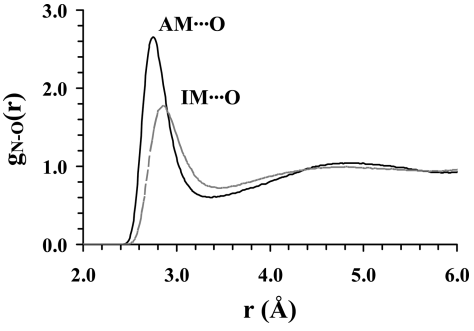

Figure 5. Partial distribution function of AM···O (black) and IM···O (gray) pairs derived from MD simulations of PAni-EB with 15% w/w of reversibly absorber water molecules. AM and IM refer to the nitrogen atom of amine and imine units, respectively, and O corresponds to the oxygen atom of TIP3P water.

shows the partial distribution function of AM···O and IM···O pairs, denoted $g_{AM\text{-}O}(r)$ and $g_{IM\text{-}O}(r)$, respectively, which have been calculated considering the distances between the oxygen atom of water molecules and the nitrogen of AM and IM units. The first peak of $g_{AM\text{-}O}(r)$ and $g_{IM\text{-}O}(r)$, which corresponds to the first hydration shell, is centered at 2.75 and 2.86 Å, respectively. This evidence that AM and IM units behave differently (i.e., IM acts as hydrogen bonding acceptor only while AM acts as both donor and acceptor), even though these hydrogen bonding distances are not consistent with those predicted by quantum mechanical calculations. The similarity of the second peak in the two partial distribution functions suggests that the second shell behave similar for AM or IM.

dx.doi.org/10.1021/jp300426b | J. Phys. Chem. B 2012, 116, 7342−7350

Figure 6a shows the probability density function of the interaction energies (ΔE_{int}) between water molecules located at a distance shorter than to 5.0 Å from the nitrogen atom of AM or IM units and the whole repeating unit associated with such nitrogen atom. ΔE_{int} values were simply estimated as the sum of simple Columbic and Lennard-Jones intermolecular potentials. The first peak corresponds to the first hydration shell with ΔE_{int} = −6.5 and −4.0 kcal/mol for AM and IM units, respectively. These values are qualitatively similar to those displayed in Table 1 and to the activation energy of 3−5 kcal/mol.[8,11] The ΔE_{int} values for the second peak (i.e., second hydration shell) reduce to −0.6 and −0.8 kcal/mol, respectively, suggesting a non-negligible attractive contribution.

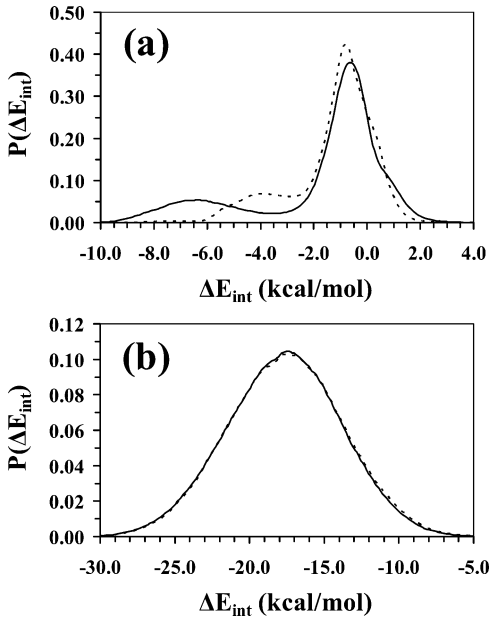

Figure 6. Probability density function of the interaction energies (ΔE_{int}) for water molecules located at a distance shorter than to 5.0 Å from the nitrogen atom of AM (solid lines) or IM units (dashed lines). The ΔE_{int} values were calculated considering the interaction between the water molecule and (a) the atoms of the repeating unit associated with the reference nitrogen atom and (b) all the atoms (i.e., PAni-EB and other water molecules) located within a cutoff distance of 15 Å with respect to the oxygen atom of the reference water.

Figure 6b represents the probability density function of ΔE_{int} considering the interaction between water molecules located at a distance shorter than to 5.0 Å from the nitrogen atom and all atoms (i.e., not only from PAni-EB but also those of other water molecules within the cutoff radius) located within a distance of 15 Å. The profiles obtained for AM and IM units are identical, the only broad peak being centered at −18.5 kcal/mol. It is worth noting that the latter value is consistent with the second activation energy reported by Matveeva et al.[8,11]

A New Hypothesis for the Organization of Water Molecules in PAni-EB. As was mentioned in the Introduction, Matveeva et al.[8,11] interpreted the thermogravimetric and calorimetric data of PAni-EB according to two types of absorbed water molecules: those hydrogen bonded to AM units with an activation energy of about 3−5 kcal/mol and the other that, after interact with the nitrogen atoms of IM units, transform into irreversibly absorbed molecules with an activation energy of about 15−18 kcal/mol. Results presented in this work allows us to propose a new hypothesis supported by quantum mechanical calculations and MD simulations, which is also compatible with those measured activation energies. Specifically, we also propose two types of physisorbed water molecules that differ in their internal organization within the polymeric matrix rather than in the binding site.

The first type of absorbed water molecules corresponds to those that are isolated with respect to other water molecules (i.e., they interact with PAni-EB but not with other water molecules, as is schematically depicted in Figure 7a). The

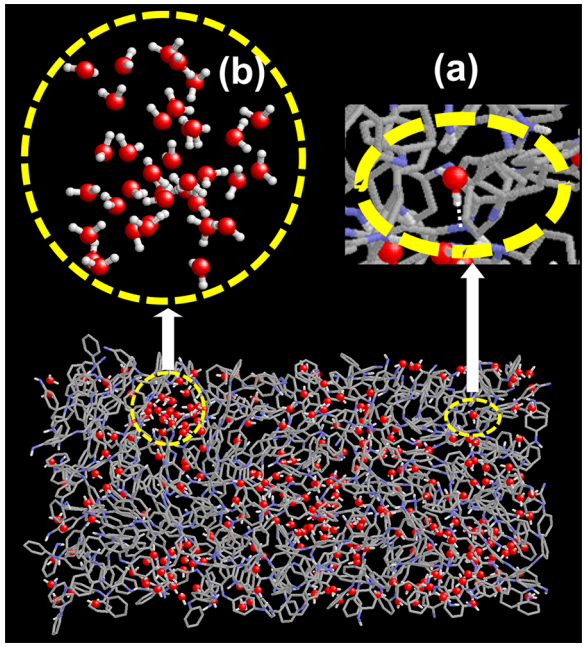

Figure 7. Schematic representation of the two types of proposed water molecules: (a) water molecules that interact individually with PAni-EB; (b) water molecules organized in nanodrops within the PAni-EB matrix.

binding energy predicted for this kind of "individual" water molecules is around 3−5 kcal/mol, independently of the binding site (i.e., AM or IM unit), in concordance with the lowest activation energy measured by Matveeva et al..[8,11] The second type of water molecules refer to those that are internally organized forming a nanodrop. These water molecules interact not only with PAni-EB chains but also with a relatively large number of surrounding water molecules. Thus, water molecules immersed in nanodrops form a dense network of cooperative intermolecular hydrogen bonds, which provide an extra stabilization. Nanodrops typically contain around 30−40 water molecules, an example being schematically represented in Figure 7b. MD simulations indicate that the binding energy of water molecules organized in nanodrops is of around −18 kcal/mol, in concordance with the highest activation energy measured by Matveeva et al.[8,11]

Figure 8 compares the radial distribution functions of intermolecular O···O atoms pairs, $g_{o\text{-}o}(r)$, where O refers to the oxygen atoms of water calculated for absorbed water and bulk pure water. The sharp and narrow peak at 2.8 Å corresponds to the first solvation shell of each water molecule. This shell is formed by the neighboring water molecules interacting thorough specific hydrogen bonds. The absence of other peaks in the $g_{o\text{-}o}(r)$ functions indicates the lack of structural organization around water molecules. The similarity

dx.doi.org/10.1021/jp300426b | J. Phys. Chem. B 2012, 116, 7342−7350

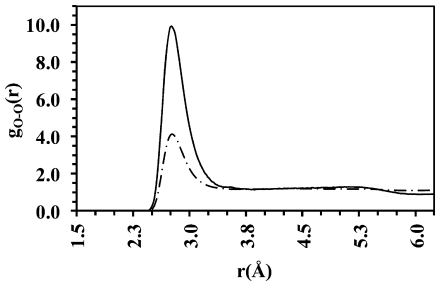

Figure 8. Partial distribution functions of the intermolecular O···O pairs, where O refers to the oxygen atom of TIP3P water, calculated for absorbed nanodrops (solid line) and bulk water (dashed line).

between the two systems provides more support to the proposed nanodrop organization.

CONCLUSIONS

Quantum mechanical calculations on model complexes indicate that the binding of a water molecule with an IM unit is slightly favored with respect to that with an AM unit. Thus, the energy gain related with the interaction between one water molecule and an AM unit is 3.0−3.7 and 4.1−4.5 kcal/mol when the nitrogen acts as hydrogen bonding acceptor and donor, respectively, this gain increasing to 6.3 kcal/mol for the interaction between one water molecule and an IM unit. These relatively small binding energies are in good agreement with the activation energies of 3−5 kcal/mol measured by Matveeva et al.,[8,11] which we attribute to reversibly absorbed water molecules that are organized individually around one AM or IM binding site.

The irreversible absorption of water has been studied using quantum mechanical calculations, FTIR spectroscopy and ^{1}H NMR. For this purpose a three steps process in which water molecules act as both acidic and nucleophilic reagent to produce C−OH groups in the attacked IM units has been considered. Calculations indicate that the successive protonation, nucleophilic attack and deprotonation steps result in a process that is thermodynamically disfavored by 5−8 kcal/mol. Although FTIR and ^{1}H NMR analyses of dehydrated and wet samples allowed us to identify reversibly absorbed water, no signal about the existence of C−OH groups was detected. These results suggest that the irreversible absorption of water molecules, which was proposed by Matveeva et al.[8,11] to explain the observed activation energy of 15−18 kcal/mol, does not occur.

Detailed energy analyses of the snapshots recorded from a MD trajectory of amorphous PAni-EB containing 15% w/w of absorbed water allow us to reinterpret the activation energies observed by Matveeva et al.[8,11] Accordingly, thermodynamic activation energies have been associated with two types of physisorbed water molecules that differ in their microscopic organization with respect to PAni-EB chains. The first one corresponds to water molecules that interact individually with PAni-EB chains while the second type refers to water molecules organized in nanodrops within the polymeric matrix. Thus, water molecules of the second type interact not only with PAni-EB chains but also with surrounding water molecules. The network of intermolecular hydrogen bonds formed by water molecules contained in the nanodrop is responsible of their high activation energy with respect to that of water molecules of the first type.

AUTHOR INFORMATION

Corresponding Author

*E-mail: carlos.aleman@upc.edu.

Notes

The authors declare no competing financial interest.

ACKNOWLEDGMENTS

Financial support from the MICINN and FEDER (MAT2009-09138 and FIS2009-13641-C02-01), Generalitat de Catalunya (research groups 2009 SGR 925 and 2009 SGR 1003, and XRQTC), CNPq (process 135245/2009-5) and CAPES (BEX 5413/10-9 and CAPES/GDU 157/08) is gratefully acknowledged. Support for the research of C.A. was received through the prize "ICREA Academia" for excellence in research funded by the Generalitat de Catalunya. Authors are indebted to the Centre de Supercomputació de Catalunya (CESCA) for the computational resources provided. Dr. Elaine Armelin is thanked for a helpful discussion.

REFERENCES

(1) Skotheim, T. A.; Reynolds, J. R. *Handbook of conducting polymers*, 3rd ed.; CRC Press: Boca Raton, 2007.
(2) Wallace, G. G.; Spinks, G. M.; Kane-Maguire, L. A. P.; Teasdale, P. R. *Conductive Electroactive Polymers*; CRC Press: Boca Raton, 2009.
(3) Freund, M. S.; Deore, B. *Self-Doped Conducting Polymers*; John Wiley & Sons Ltd.: West Sussex, England, 2007.
(4) Epstein, A. J.; Ginder, J. M.; Zuo, F.; Bigelow, R. W.; Hoo, H. S.; Tanner, D. B.; Richter, A. F.; Huang, W. S.; MacDiarmid, A. G. *Synth. Met.* **1987**, *18*, 303.
(5) Joo, J.; Epstein, A. J.; Prigodin, V. N.; Min, G. Y.; MacDiarmid, A. G. *Phys. Rev. B* **1994**, *50*, 1226.
(6) Lu, W.; Fadeev, A. G.; Qi, B.; Smela, E.; Mattes, B. R.; Ding, J.; Spinks, G. M.; Mazurkiewcz, J.; Zhou, D.; Wallace, G. G.; MacFarlane, D. R.; Forsyth, S. A.; Forsyth, M. *Science* **2002**, *297*, 983.
(7) Alix, A.; Lemoine, V.; Nechtschein, M.; Travers, J. P.; Menardo, C. *Synth. Met.* **1989**, *29*, 457.
(8) Matveeva, E. S.; Díaz Calleja, R.; Parkhutik, V. P. *Synth. Met.* **1995**, *72*, 105.
(9) Lubentsov, B. Z.; Timofeeva, O. N.; Khidekel, M. L. *Synth. Met.* **1991**, *45*, 235.
(10) Lubentsov, B. Z.; Timofeeva, O. N.; Saratovskikh, S.; Krinichnyi, V.; Pelekh, A.; Dmitrenko, V.; Khidekel, M. *Synth. Met.* **1992**, *47*, 187.
(11) Matveeva, E. S. *Synth. Met.* **1996**, *79*, 127.
(12) Rodrigues, P. C.; de Souza, G. P.; Da Motta Neto, J. D.; Akcelrud, L. *Polymer* **2002**, *43*, 5493.
(13) Canales, M.; Aradilla, D.; Alemán, C. *J. Polym. Sci., Part B: Polym. Phys.* **2011**, *49*, 1322.
(14) Gaussian 09, Revision A.02, Frisch, M. J.; Trucks, G. W.; Schlegel, H. B.; Scuseria, G. E.; Robb, M. A.; Cheeseman, J. R.; Scalmani, G.; Barone, V.; Mennucci, B.; Petersson, G. A.; Nakatsuji, H.; Caricato, M.; Li, X.; Hratchian, H. P.; Izmaylov, A. F.; Bloino, J.; Zheng, G.; Sonnenberg, J. L.; Hada, M.; Ehara, M.; Toyota, K.; Fukuda, R.; Hasegawa, J.; Ishida, M.; Nakajima, T.; Honda, Y.; Kitao, O.; Nakai, H.; Vreven, T.; Montgomery, J. A., Jr.; Peralta, J. E.; Ogliaro, F.; Bearpark, M.; Heyd, J. J.; Brothers, E.; Kudin, K. N.; Staroverov, V. N.; Kobayashi, R.; Normand, J.; Raghavachari, K.; Rendell, A.; Burant, J. C.; Iyengar, S. S.; Tomasi, J.; Cossi, M.; Rega, N.; Millam, J. M.; Klene, M.; Knox, J. E.; Cross, J. B.; Bakken, V.; Adamo, C.; Jaramillo, J.; Gomperts, R.; Stratmann, R. E.; Yazyev, O.; Austin, A. J.; Cammi, R.; Pomelli, C.; Ochterski, J. W.; Martin, R. L.; Morokuma, K.; Zakrzewski, V. G.; Voth, G. A.; Salvador, P.; Dannenberg, J. J.; Dapprich, S.; Daniels, A. D.; Farkas, O.; Foresman, J. B.; Ortiz, J. V.; Cioslowski, J.; Fox, D. J. Gaussian, Inc.: Wallingford CT, 2009.
(15) (a) Becke, A. D. *J. Chem. Phys.* **1993**, *98*, 1372. (b) Lee, C.; Yang, W.; Parr, R. G. *Phys. Rev. B* **1988**, *37*, 785.

(16) McLean, A. D.; Chandler, G. S. *J. Chem. Phys.* **1980**, *72*, 5639.
(17) Boys, S. F.; Bernardi, F. *Mol. Phys.* **1970**, *19*, 553.
(18) Canales, M.; Curcó, D.; Alemán, C. *J. Phys. Chem. B* **2010**, *114*, 9771.
(19) Pouget, J. P.; Jozefowicz, M. E.; Epstein, A. J.; Tang, X.; MacDiarmid, A. G. *Macromolecules* **1991**, *24*, 779.
(20) Jorgensen, W. L.; Chandrasekhar, J.; Madura, J. D.; Impey, R. W.; Klein, M. L. *J. Chem. Phys.* **1983**, *79*, 926.
(21) Darden, T.; York, D.; Pedersen, L. *J. Chem. Phys.* **1993**, *98*, 10089.
(22) Berendsen, H. J. C.; van der Spoel, D.; van Drunen, R. *Comput. Phys. Commun.* **1995**, *91*, 43.
(23) Lindahl, E.; Hess, B.; van der Spoel, D. *J. Mol. Model.* **2001**, *7*, 306.
(24) Van Der Spoel, D.; Lindahl, E.; Hess, B.; Groenhof, G.; Mark, A. E.; Berendsen, H. J. C. *J. Comput. Chem.* **2005**, *26*, 1701.
(25) Hess, B.; Kutzner, C.; van der Spoel, D.; Lindahl, E. *J. Chem. Theory Comput.* **2008**, *4*, 435.
(26) Berendsen, H. J. C.; Postma, J. P. M.; van Gunsteren, W. F.; DiNola, A.; Haak, J. R. *J. Chem. Phys.* **1984**, *81*, 3684.
(27) Alemán, C.; Namba, A. M.; Casanovas, J. *J. Biomol. Struct. Dyn.* **2005**, *23*, 29.
(28) Ilic, M.; Koglin, A.; Pohlmeier, H. D.; Narres, H. D.; Schwuger, M. *Langmuir* **2000**, *16*, 8946.
(29) Trchová, M.; Stejskal, J. *Pure Appl. Chem.* **2011**, *83*, 1803.
(30) Kang, E. T.; Neoh, K. G.; Tan, K. L. *Prog. Polym. Sci.* **1998**, *23*, 277.
(31) Yelil-Arasi, A.; Latha-Jeyakumari, J. J.; Sundaresan, B.; Dhanalakshmi, V.; Anbarasan, R. *Spectrochim. Acta Part A* **2009**, *74*, 1229.
(32) Wang, X.; Sun, T.; Wang, C.; Wang, C.; Zhang, W.; We, Y. *Macromol. Chem. Phys.* **2010**, *211*, 1814.
(33) Spectral Database for Organic Compounds (SBDS). http://riodb01.ibase.aist.go.jp/sdbs/cgi-bin/cre_index.cgi